JACS
JOURNAL OF THE AMERICAN CHEMICAL SOCIETY
Communication
pubs.acs.org/JACS

Magic Angle Spinning and Oriented Sample Solid-State NMR Structural Restraints Combine for Influenza A M2 Protein Functional Insights

Thach V. Can,[†,∥] Mukesh Sharma,[‡,#] Ivan Hung,[‡] Peter L. Gor'kov,[‡] William W. Brey,[‡] and Timothy A. Cross*[,‡,§,⊥]

[†]Department of Physics, [§]Department of Chemistry and Biochemistry, and [⊥]Institute of Molecular Biophysics, Florida State University, Tallahassee, Florida 32306, United States

[‡]National High Magnetic Field Laboratory, Florida State University, Tallahassee, Florida 32310, United States

Supporting Information

ABSTRACT: As a small tetrameric helical membrane protein, the M2 proton channel structure is highly sensitive to its environment. As a result, structural data from a lipid bilayer environment have proven to be essential for describing the conductance mechanism. While oriented sample solid-state NMR has provided a high-resolution backbone structure in lipid bilayers, quaternary packing of the helices and many of the side-chain conformations have been poorly restrained. Furthermore, the quaternary structural stability has remained a mystery. Here, the isotropic chemical shift data and interhelical cross peaks from magic angle spinning solid-state NMR of a liposomal preparation strongly support the quaternary structure of the transmembrane helical bundle as a dimer-of-dimers structure. The data also explain how the tetrameric stability is enhanced once two charges are absorbed by the His37 tetrad prior to activation of this proton channel. The combination of these two solid-state NMR techniques appears to be a powerful approach for characterizing helical membrane protein structure.

The M2 protein from Influenza A is an important drug target and has been the subject of numerous structural efforts. The protein has shown a high degree of structural sensitivity to the sample environment, hence the need to pursue studies in an environment similar to that of the native membrane.[1] As a tetramer, M2 forms a proton channel that shuttles protons across the membrane. The channel has a primary gate formed by four Trp41 residues and a secondary gate formed by four Val27 residues near the entrance to the pore.[2,3] Shuttling is achieved by a tetrad of His37 residues once activated by binding a third proton and hence a third charge.[4] An amphipathic helix at the C-terminus of the transmembrane (TM) pore is associated with viral budding resulting from its insertion into the lipid interface.[5] This helix is also necessary for achieving native conductance properties of the full-length protein.[6] It is important to note that M2 functions at the neck of the viral bud[5] and consequently does not appear to be solubilized and functioning in the high-cholesterol/sphingomyelin membrane environment that dominates the viral envelope. Consequently, we continue to study M2 in lipids that form liquid crystalline environments. Here, magic angle spinning solid-state NMR (MAS ssNMR) provides numerous structural restraints in the same lipid environment used for oriented sample (OS) ssNMR spectroscopy that provided a high-resolution backbone structure of the M2 conductance domain (residues 22−62), including both the TM and amphipathic helices.[7] The MAS chemical shift data and distance restraints provide unique insights into the stability of this tetrameric structure and the functionality of the histidine tetrad.

Early backbone structures of the M2 TM domain (residues 22−46) in lipid bilayers were achieved by OS ssNMR without (PDB 1NYJ) and with (PDB 2H95) the antiviral drug amantadine.[8,9] This latter structure was refined recently with MAS ssNMR data by Hong and co-workers (PDB 2KQT).[10] Crystal structures of the TM domain in detergent environments have also been achieved in recent years with and without amantadine (PDB 3BKD, 3C9J, 3LBW).[11,12] In this same time frame, solution NMR structures of the conductance domain (residues 18−60) in detergent micelles were achieved (PDB 2RLF, 2KIH, 2KWX),[13,14] along wth the recent OS ssNMR structure of the conductance domain in liquid crystalline bilayers (PDB 2L0J).[7]

The backbone structure of the TM domain has progressed toward a consensus. Functionally important details of the conserved HxxxW and the amphipathic helices elucidated in lipid bilayers, however, have not achieved such consensus. In 2006, the pK_a values of the histidine tetrad were determined, identifying a very high proton and charge affinity by this channel with two pK_a values at 8.2.[4] The much higher than normal proton affinity suggests that the structure is stabilized by these charges, yet His37 is in the low dielectric environment near the center of the membrane, suggesting substantial charge−charge repulsion for these closely packed charges. Such repulsion would destabilize the tetrameric structure, but it has been shown that at pH 6.5, where the histidine tetrad carries two charges, the tetramer is much more stable.[6] It has been suggested that the charges may be extensively delocalized over a dimer-of-dimers structure.[7,15] Two identical pK_a values further suggest cooperative proton binding and hence a

Received: January 13, 2012
Published: May 22, 2012

   dx.doi.org/10.1021/ja3004039 | J. Am. Chem. Soc. 2012, 134, 9022−9025

conformational change following the binding of the first proton to the histidine tetrad, but the conformational change associated with cooperative binding has not been previously identified.

None of the solution NMR or crystal structures in a detergent environment, nor the ssNMR data obtained from M2 in a cholesterol- and sphingomyelin-rich environment,[16,17] have shown this dimer-of-dimers configuration with imdazole–imidazolium hydrogen bonding as described in the OS ssNMR structure. However, Griffin and co-workers recently published MAS ssNMR data obtained from frozen and specifically labeled samples that show multiple backbone sites generating resonance pairs including His37 and Trp41.[15] In so doing, the dimer-of-dimers conformation for the HxxxW tetrad was confirmed, and they further suggest that the dimerization extends throughout the TM domain.

NCOCX and NCACX 3D data sets were recorded for the M2 conductance domain in a pH 7.5 preparation of DOPC/DOPE (4:1 molar ratio) liposomes, representing the same model membrane environment as that used for the OS ssNMR (sample and spectroscopic details in the SI). Sample assignment strips are shown in Figure S1, and the resonance assignments for the TM helix are presented in Table S1. These assignments are consistent with the selective ^{15}N- and ^{13}C-labeling results from the Griffin and Hong laboratories when lipid bilayers capable of forming liquid crystalline environments have been used. The resonances in the TM helix are significantly narrower than those in the amphipathic helix, and hence we have focused the data analysis effort here on the TM helix.

TALOS+[18] was used to calculate the backbone torsion angles from the backbone chemical shifts for an 18-residue stretch from Leu26 through Leu43. The predictions (Table S2) generated average ϕ,ψ angles of −62.8°,−41.7° that are remarkably close to the average ϕ,ψ angles in 2L0J, which for the same residues are −60.9°,−43.5°. The OS ssNMR values are closer to those expected for TM helices (ϕ = −60°, ψ = 45°), for which intrahelical hydrogen bonding is stronger.[19]

Figure 1 displays the aliphatic cross peaks to carbonyl, aromatic, and aliphatic sites at various mixing times for ^{13}C–^{13}C correlation spectra of M2 22–62 (see SI for details).

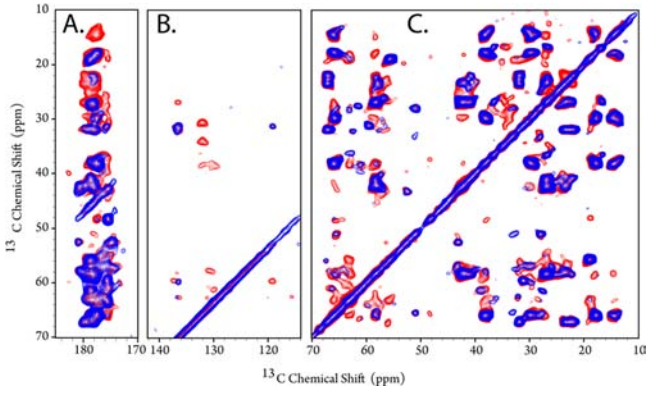

Figure 1. ^{13}C–^{13}C correlation spectral regions obtained from a liposomal preparation of M2 22–62. All spectra were obtained at 600 MHz using a ^{13}C-optimized ^{1}H/^{13}C/^{15}N 3.2 mm biosolids MAS probe with Low-E coil technology.[20,21] (A) Carbonyl–aliphatic region, 9 (blue) and 50 ms (red) mixing times; (B) aromatic–aliphatic region, 9 (blue) and 100 ms (red) mixing times; (C) aliphatic–aliphatic region, 20 (blue) and 50 ms (red) mixing times.

These spectra immediately identify a major challenge for MAS spectroscopy of α-helical membrane proteins. The chemical shifts of the hydrophobic side chains have remarkably little dispersion. This, coupled with the fact that of the 21 residues in the M2 TM helix (residues 26–46), 15 are either alanine (2), valine (2), isoleucine (5), or leucine (6) residues, makes it very challenging to uniquely interpret cross peaks involving these resonance clusters. The 1 ppm average ^{13}C line widths are excellent for liposome preparations. Overall, it would be very difficult to achieve a well-restrained structure from these spectra alone in this native-like liposome environment. While the backbone structure of the conductance domain as well as the helical tilt and rotation angles were determined to high resolution by orientational restraints, limited data were available for the side-chain conformations and the quaternary structure. Fortunately, there are multiple unique residues in the TM helix: Ser31, Gly34, His37, Trp41, Asp44, and Arg45 that are resolved and uniquely assigned and can be used for obtaining distance restraints from the MAS ^{13}C–^{13}C correlation spectra.

Six unique interhelical restraints were obtained from mixing times between 20 and 200 ms. These restraints and their multiplicity in this tetrameric structure are tabulated in Table S3 and illustrated in Figure 2. In 2L0J, the Ser31 and Ala30 Cβ groups are in van der Waals contact via interhelical packing while considerably separated in their intrahelical interactions; therefore, the cross peak (18.8 and 63.2 ppm) that is visible in the 20 and 50 ms spectra (Figure 1C) is assigned to the four-fold symmetric interhelical distance. The remaining unique cross peaks leading to distance restraints were observed through His37 and mostly from HisB/D (chains B and D). The two sets of His37 side-chain resonances (forming a dimer-of-dimers conformation) have greater (HisB/D: Cα 59.5, Cβ 31.1, Cγ 137.3, Cδ2 119.4, Cε1 136.4 ppm) and lesser (HisA/C: Cα 62.4, Cβ 32.1, Cγ 131.0, Cδ2 115.6, Cε1 136.7 ppm) fractional charge, consistent with the histidine titration data.[22] These chemical shifts provide an opportunity to observe cross peaks between the His37 residues as well as unique cross peaks from His37 to other side chains.

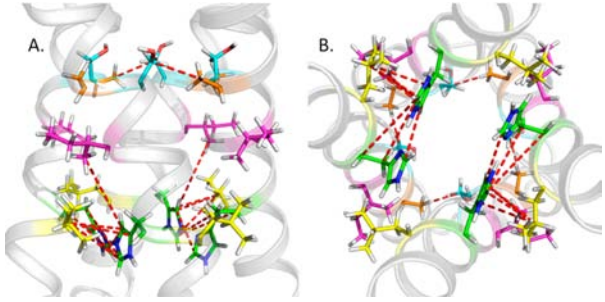

Figure 2. Distance restraints (red dashed lines) in the TM region of the M2 protein. Carbon colors: Ala30, brown; Ser31, cyan; Ile33, magenta; His37, green; and Leu38, yellow. (A) Side view of the structure; (B) view down the pore axis from the C-terminal end of the TM helix.

The dynamics of the two imidazoles in each pair appear to be quite different. For HisB/D, the Nε2 donates a hydrogen bond to HisA/C Nδ1, and in addition the Nδ1H of HisB/D forms an intraresidue electrostatic interaction with the backbone carbonyl, thereby significantly stabilizing the HisB/D side chain. The HisA/C Nε2H forms an interaction with the π electron density of the Trp41 indole rings, but this interaction does not strongly

dx.doi.org/10.1021/ja3004039 | J. Am. Chem. Soc. 2012, 134, 9022–9025

restrain either $\chi 1$ or $\chi 2$ because of the expanse of indole π electron density. In the $^{13}C-^{13}C$ correlation spectra the spectral intensities for HisB/D are significantly stronger and are also observed at longer mixing times than those for HisA/C. In particular, the Cδ2 of HisA/C displays only weak signals in these samples. Similarly, all of the Trp41 indole cross peak intensities are very weak, and in the aromatic cross peak region the resonances mostly disappear for mixing times of 100 ms or greater. The implied dynamics for the Trp41 indoles further corroborate the previous conclusion about the dynamics of the His37A/C that interacts with Trp41.[7]

In addition to the cross peaks between Ala30 and Ser31, and between imidazole (HisA/C) and imidazolium (HisB/D), HisB/D displays cross peaks with Leu38A/C and Ile 33B/D. Each of these distance restraints is two-fold symmetric, resulting in a total of 16 restraints, with 14 of them being interhelical for the quaternary structure. Three of the unique distance restraints are from His 37B/D Cγ, Cδ2, and Cε1 to a Leu Cγ. While the Leu resonance assignments have some ambiguity, the distances in 2L0J show that Leu38A/C provides the shortest distances (by ~2 Å) to His37B/D and hence the specific assignment for these distances. In addition to the helical structure and its orientation relative to its environment from orientational restraints, these distance restraints provide additional restraints to precisely define the quaternary structure of the TM domain (Figure 2). This quaternary structure is consistent with both the OS ssNMR structure (2L0J) and the recent X-ray crystal structure of the TM domain (3LBW); however, the Ala30−Ser31 distance is inconsistent with the solution NMR structures (2RLF, 2KWX)[13,14] that have somewhat different helical packing near the N-terminus.

The two sets of resonances observed for the His37 residues support the unique imidazole−imidazolium dimer arrangement based on the pH titration of the Nδ1- and Nε2-labeled M2 TM domain that defined a strong Nδ1−H−Nε2 hydrogen bond between these side chains.[4] The differences in chemical shifts between the charged histidine amino acid and neutral ε2 protonated tautomer for the Cδ2 (5.8 ppm), Cγ (−9.0 ppm), and Cε1 (1.0 ppm) sites[22] are significantly larger than the chemical shift differences observed between HisB/D and HisA/C in the M2 22−62 Cδ2 (3.8 ppm), Cγ (−6.3 ppm), and Cε1 (−0.3 ppm) sites reported here. This reduction in the chemical shift differences suggests that the Coulombic charge is not localized to a single imidazole but is dispersed as hypothesized based on the need for minimizing the electrostatic repulsion.[4,7] At the same time the unique chemical shifts for these two His37 side chains rule out four-fold symmetric structures, such as the recent crystal structure (3LBW). However, the M2 solution NMR structures represent time-averaged structures at 303 K and consequently may reflect an average of the two conformations. Figure 3 shows a comparison of the $^{13}C-^{13}C$ correlation spectra for M2 22−62 at pH 7.5 and 6.0, illustrating that there is no significant change in the Cα and Cβ chemical shifts of His37 and Trp41 over this pH range. Consequently, there does not appear to be a change in the ionization state over this pH range. Previously the third pK_a was characterized from the TM domain (residues 22−46) samples as being 6.3. It has been documented by analytical ultracentrifugation that the TM domain has much lower structural stability (via K_{app}) than the full-length protein.[6] Consequently, we anticipate that, for the conductance domain and full-length protein, the third pK_a will be lower than pH 6.3.

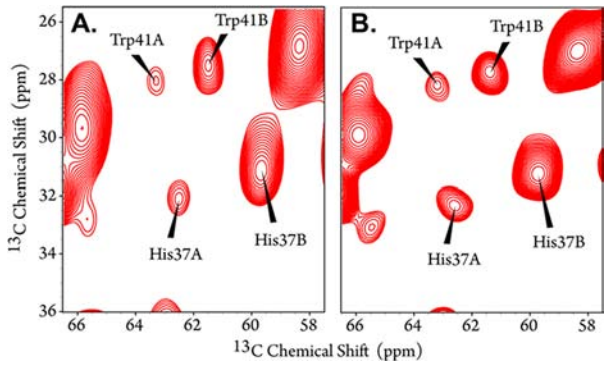

Figure 3. $^{13}C-^{13}C$ correlation spectra from liposomal preparations of M2 22−62. (A) pH 6.0, 9 ms mixing; (B) pH 7.5, 20 ms mixing. Otherwise as described in Figure 1.

The assigned chemical shifts for the His37 residues and distance restraints involving these residues support the unique histidine tetrad structure in 2L0J. The formation of imidazole−imidazolium hydrogen bonds explains analytical ultracentrifugation data showing that the tetrameric stability increases as the pH is lowered from 9 to 6.5, by 3 orders of magnitude for the full-length protein.[6] Without these H-bonds it is not possible to explain the increased stability while charge repulsion is increased due to the addition of two charges in the histidine tetrad.

As suggested previously,[7] the dimer-of-dimers conformation formed by the imidazole−imidazolium H-bonds may undergo conformational exchange in which the pairs of imidazoles sharing a H-bond exchange with those that do not share a H-bond. The recent four-fold symmetric crystal structure has Cα carbons separated by 8.6 and 8.7 Å, while the separation of Cα carbons in a QM/MM refined imidazole−imidazolium pair for the 2L0J structure is 9.0−9.1 Å. It appears that the formation of the imidazole−imidazolium H-bond forces the backbone apart and, in so doing, facilitates the binding of the second proton, hence the cooperativity in binding the first two protons to the histidine tetrad. The structure suggests that the separation of His37 Cα carbons that do not form imidazole−imidazolium pairs could be significantly less than 9.0 Å, resulting in a rectangular placement of the Cα carbons. This could explain the data supporting a dimer-of-dimers structure that is observed for many sites in the polypeptide backbone.[15]

The unique histidine tetrad forms a dimer-of-dimers conformation so that two charges can be stabilized in the middle of the lipid bilayer in this small helical bundle. Charge repulsion is minimized by an Nδ1−H Nε2 hydrogen moving back and forth over a low-energy barrier between two imidazoles. Here, it is also apparent that the charge is not equally distributed over the two rings, but the proton resides preferentially with the Nε2 site, consistent with the known propensity for Nε2 to bind protons preferentially over Nδ1.[22]

MAS and OS ssNMR spectroscopies are highly complementary. Here, the same sample preparation used previously for the OS ssNMR samples has been used for the MAS samples. The combination of orientational and distance restraints take advantage of both approaches and eliminates the need to completely define the structure using one approach. Considering the lack of MAS spectral dispersion for α-helical membrane proteins and the difficulty in characterizing the aliphatic side chains with OS ssNMR, this combination represents a powerful approach. Here, numerous interhelical

dx.doi.org/10.1021/ja3004039 | J. Am. Chem. Soc. 2012, 134, 9022−9025

restraints as well as isotropic chemical shift data from MAS ssNMR spectroscopy were obtained that constrain the tetrameric structure. These restraints have allowed us to significantly advance our knowledge of the structure, dynamics, and functionality of this important drug target.

■ ASSOCIATED CONTENT

Supporting Information

Experimental procedures, spectroscopic data, and data tables. This material is available free of charge via the Internet at http://pubs.acs.org.

■ AUTHOR INFORMATION

Corresponding Author

cross@magnet.fsu.edu

Present Addresses

[‖]Department of Physics, Cornell University, Ithaca, NY 14853
[#]Department of Biological Chemistry & Molecular Pharmacology, Harvard Medical School, Boston, MA 02115

Notes

The authors declare no competing financial interest.

■ ACKNOWLEDGMENTS

This work was supported in part by the National Institutes of Health Grant AI23007 and conducted at the National High Magnetic Field Laboratory supported by Cooperative Agreement 0654118 between the Division of Materials Research of the National Science Foundation and the State of Florida.

■ REFERENCES

(1) Cross, T. A.; Sharma, M.; Yi, M.; Zhou, H. X. *Trends Biochem. Sci.* **2011**, *36*, 117.
(2) Tang, Y.; Zaitseva, F.; Lamb, R. A.; Pinto, L. H. *J. Biol. Chem.* **2002**, *277*, 39880.
(3) Yi, M.; Cross, T. A.; Zhou, H. X. *J. Phys. Chem. B* **2008**, *112*, 7977.
(4) Hu, J.; Fu, R.; Nishimura, K.; Zhang, L.; Zhou, H. X.; Busath, D. D.; Vijayvergiya, V.; Cross, T. A. *Proc. Natl. Acad. Sci. U.S.A.* **2006**, *103*, 6865.
(5) Rossman, J. S.; Jing, X.; Leser, G. P.; Lamb, R. A. *Cell* **2010**, *142*, 902.
(6) Ma, C.; Polishchuk, A. L.; Ohigashi, Y.; Stouffer, A. L.; Schon, A.; Magavern, E.; Jing, X.; Lear, J. D.; Freire, E.; Lamb, R. A.; DeGrado, W. F.; Pinto, L. H. *Proc. Natl. Acad. Sci. U.S.A.* **2009**, *106*, 12283.
(7) Sharma, M.; Yi, M.; Dong, H.; Qin, H.; Peterson, E.; Busath, D. D.; Zhou, H. X.; Cross, T. A. *Science* **2010**, *330*, 509.
(8) Nishimura, K.; Kim, S.; Zhang, L.; Cross, T. A. *Biochemistry* **2002**, *41*, 13170.
(9) Hu, J.; Asbury, T.; Achuthan, S.; Li, C.; Bertram, R.; Quine, J. R.; Fu, R.; Cross, T. A. *Biophys. J.* **2007**, *92*, 4335.
(10) Cady, S. D.; Schmidt-Rohr, K.; Wang, J.; Soto, C. S.; Degrado, W. F.; Hong, M. *Nature* **2010**, *463*, 689.
(11) Stouffer, A. L.; Acharya, R.; Salom, D.; Levine, A. S.; Di Costanzo, L.; Soto, C. S.; Tereshko, V.; Nanda, V.; Stayrook, S.; DeGrado, W. F. *Nature* **2008**, *451*, 596.
(12) Acharya, R.; Carnevale, V.; Fiorin, G.; Levine, B. G.; Polishchuk, A. L.; Balannik, V.; Samish, I.; Lamb, R. A.; Pinto, L. H.; DeGrado, W. F.; Klein, M. L. *Proc. Natl. Acad. Sci. U.S.A.* **2010**, *107*, 15075.
(13) Schnell, J. R.; Chou, J. J. *Nature* **2008**, *451*, 591.
(14) Pielak, R. M.; Chou, J. J. *Biochem. Biophys. Res. Commun.* **2010**, *401*, 58.
(15) Andreas, L. B.; Eddy, M. T.; Pielak, R. M.; Chou, J.; Griffin, R. G. *J. Am. Chem. Soc.* **2010**, *132*, 10958.
(16) Hu, F.; Luo, W.; Hong, M. *Science* **2010**, *330*, 505.
(17) Hu, F.; Schmidt-Rohr, K.; Hong, M. *J. Am. Chem. Soc.* **2012**, *134*, 3703.
(18) Shen, Y.; Delaglio, F.; Cornilescu, G.; Bax, A. *J. Biomol. NMR* **2009**, *44*, 213.
(19) Page, R. C.; Kim, S.; Cross, T. A. *Structure* **2008**, *16*, 787.
(20) Gor'kov, P. L.; Chekmenev, E. Y.; Li, C.; Cotten, M.; Buffy, J. J.; Traaseth, N. J.; Veglia, G.; Brey, W. W. *J. Magn. Reson.* **2007**, *185*, 77.
(21) McNeill, S. A.; Gor'kov, P. L.; Shetty, K.; Brey, W. W.; Long, J. R. *J. Magn. Reson.* **2009**, *197*, 135.
(22) Li, S.; Hong, M. *J. Am. Chem. Soc.* **2011**, *133*, 1534.